JOURNAL OF PHYSICAL ORGANIC CHEMISTRY
J. Phys. Org. Chem. 2001; **14:** 811–818
DOI:10.1002/poc.436

Structural study of ethyl 3-arylcarbamoyl-2,3-diazabicyclo[2.2.1]hept-5-ene-2-carboxylates: conformation and transmission of substituent effects across the diazabicycloheptene ring†

A. Perjéssy,[1]* P. Meyer,[2] W.-D. Rudorf,[2] D. Loos,[1] E. Kolehmainen,[3] K. Laihia,[3] M. Nissinen,[3] J. Koivisto[3] and R. Kauppinen[3]

[1]Department of Organic Chemistry and Institute of Chemistry, Faculty of Natural Sciences, Comenius University, SK-84215 Bratislava, Slovak Republic
[2]Institute of Organic Chemistry, Martin Luther University, D-06099 Halle (Saale), Germany
[3]Department of Chemistry, University of Jyväskylä, PO Box 35, FIN-40351 Jyväskylä, Finland

Received 17 April 2001; revised 10 July 2001; accepted 16 July 2001

epoc ABSTRACT: Nine new ethyl 3-arylcarbamoyl-2,3-diazabicyclo[2.2.1]hept-5-ene-2-carboxylates were prepared by a [4 + 2] cycloaddition and their FTIR, ^{1}H, ^{13}C and ^{15}N NMR spectra were measured and assigned. Single crystals were grown for five compounds and their X-ray data were obtained. The electronic structure and the conformations were calculated by the semi-empirical AM1 method. Using correlations between the spectral, empirical and theoretical structural data, the transmission of substituent effects and the preferential conformation connected with the consecutive double nitrogen inversion and regarding the mutual orientation of N—H and C═O bonds were investigated. The results are compared with those for a previously reported series of analogous ethyl 2-arylcarbamoyl-4,5-dimethyl-1,2,3,6-tetrahydropyridazine-1-carboxylates. Copyright © 2001 John Wiley & Sons, Ltd.
Additional material for this paper is available from the epoc website at http://www.wiley.com/epoc

KEYWORDS: ethyl 3-arylcarbamoyl-2,3-diazabicyclo[2.2.1]hept-5-ene-2-carboxylates; FTIR, ^{1}H, ^{13}C and ^{15}N NMR spectra; AM1 and X-ray data; conformation; transmission of substituent effects

INTRODUCTION

Diaza compounds, in general, are starting materials for the synthesis of compounds with potential biological activity. They have been used as key intermediates in the preparation of 4-piperidazinethiols, which are efficient antiradiation agents.[1] Other derivatives are interesting as prostaglandin endoperoxide analogues[2] or show significant insecticidal activity.[3] Diels–Alder reaction[4] of azo compounds with cyclopentadiene leads in a [4 + 2] cycloaddition to 2,3-diazabicyclo[2.2.1]hept-5-enes. Such syntheses were reported,[5–7] but there are only a few cases using unsymmetrically substituted azo compounds.[8–10] The conformational flexibility, the mechanism of interconversion and the biochemistry of various cyclic diaza compounds make their structures interesting to study.[11–14] Therefore, analogously to the previously described procedure,[11] in a one-pot reaction, ethyl 2-arylcarbamoylhydrazino-1-carboxylates were oxidized with lead(IV) acetate to form non-isolated azo compounds that reacted smoothly with cyclopentadiene leading to ethyl 3-arylcarbamoyl-2,3-diazabicyclo-[2.2.1]hept-5-ene-2-carboxylates (**1a–1i**). We found, that compounds **1** react by intramolecular cyclization leading to ring-fused triazolidinediones, which are good herbicides;[15] see also the previously reported examples.[16–18]

The aim of the present work was to study the FTIR and NMR spectra as well as the X-ray structure and AM1 theoretical data for a series of unreported *N*,*N*′-disubstituted 2,3-diazabicyclo-[2.2.1]hept-5-enes (**1a–1i** in Scheme 1) and compare them with those reported previously[11,12] for a series of *N*,*N*′-disubstituted 4,5-dimethyl-1,2,3,6-tetrahydropyridazines (**2a–2k** in Scheme 1). The study of the conformation and the transmission of substituent effects was also an important target of this paper.

**Correspondence to:* A. Perjéssy, Department of Organic Chemistry, Faculty of Natural Sciences, Comenius University, Mlynská dolina CH-2, SK-84215 Bratislava, Slovak Republic.
E-mail: perjessy@fns.uniba.sk
†Dedicated to Dr John Shorter on the occasion of his 75th birthday.
Contract/grant sponsor: Bundesministerium für Bildung and Forschung beim DLR.
Contract/grant sponsor: Slovak Ministry of Education.
Contract/grant sponsor: Scientific Grant Agency of Ministry of Education of Slovak Republic; *Contract/grant number:* 1/7339/20.

Table 1. Wavenumbers (cm^{-1}) of IR stretching vibrations for compounds **1**

	$CHCl_3$				CCl_4			
Compound	$\nu(C_8{=}O)$	$\nu(C_5{=}C_6)$	$\nu(C_9{=}O)$	$\nu(N_{10}{-}H)$	$\nu(C_8{=}O)$	$\nu(C_5{=}C_6)$	$\nu(C_9{=}O)$	$\nu(N_{10}{-}H)$
1a	1683.8	1715.5	1727.2	3415.1	1696.5	1712.9	1724.7	3428.7
1b	1687.1	1717.9	1729.6	3414.5	1698.2	1713.5	1723.6	3427.3
1c	1687.5	1716.8	1727.1	3412.7	1697.9	1714.0	1726.4	3426.9
1d	1686.0	1714.5	1715.7	3411.0	1697.7	1714.1	1726.0	3426.9
1e	1686.8	1714.6	1715.3	3411.2	1699.0	1714.5	1727.0	3425.9
1f	1689.4	1712.3	1721.6	3410.1	1699.1	1713.4	1726.3	3423.4
1g	1689.6	1710.8	1722.9	3409.1	1698.7	1713.2	1728.2	3423.5
1h	1690.3	1710.5	1724.4	3405.0	1698.9	1713.3	1731.1	3419.4
1i	1695.9	1718.3	1724.2	3399.6	1702.0	1714.9	1732.3	3415.2

RESULTS AND DISCUSSION

The wavenumbers of the C=O, C=C and N—H IR stretching vibrations for the series of compounds **1** measured in $CHCl_3$ and CCl_4 are listed in Table 1. The IR spectra of these compounds strongly resemble those of the analogous tetrahydropyridazine derivatives **2**. However, the wavenumbers of the $\nu(C_5{=}C_6)$ vibration are always more than 20 cm^{-1} higher than in the case of compounds **2**. This is caused by the increased strain in the five-membered ring of the bicyclic system of **1**. On the other hand, the same effect causes a moderate decrease in the wavenumbers of the $\nu(C_9{=}O)$ and $\nu(N_{10}{-}H)$ vibrations of **1**. The exceptions are the wavenumbers of the $\nu(C_8{=}O)$ vibrations in $CHCl_3$, which e.g. for **1e** is by 13 cm^{-1} higher than that for the monocyclic analogue **2** (X=H).[11] This can be accounted for the steric effect of the bridging CH_2 group in the bicyclic system, which partly hinders the weak hydrogen bonding solvent effect of the $CHCl_3$ molecules on the amidic carbonyl group. The proximity of these groups are evident also from the measured and calculated interatomic distances $H_7\cdots O_8$ (see Table 5).

In elucidation of the NMR spectra different 2D correlation techniques, such as pulsed field gradient (PFG) heteronuclear multiple-quantum correlation (HMQC) and heteronuclear multiple-bond connectivities (HMBC) were used. The ^1H NMR spectrum of the parent compound (**1e**) was analysed using PERCH software.[19] The ^1H, ^{13}C and ^{15}N NMR chemical shifts of compounds **1a–1i** are presented in Tables 2–4. The results of the ^1H NMR spectrum analysis with PERCH software for compound **1e** are listed in Table 1 of the supplementary material on the EPOC website (http://www.wiley.com/epoc).

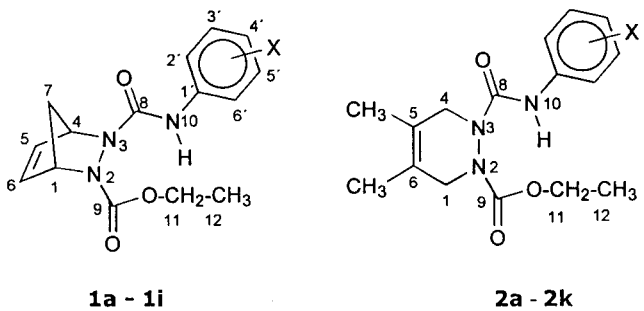

Scheme 1. X: **1a**, 4-OCH_3; **1b**, 4-CH_3; **1c**, 4-C_2H_5; **1d**, 3-CH_3; **1e**, H; **1f**, 4-Cl; **1g**, 4-Br; **1h**, 3,4-Cl_2; **1i**, 4-NO_2; **2a**, 4-CH_3; **2b**, 2-CH_3; **2c**, 4-C_2H_5; **2d**, 3-CH_3; **2e**, H; **2f**, 4-Cl; **2g**, 4-Br; **2h**, 3-Cl; **2i**, 4-OCH_3; **2j**, 4-NO_2; **2k**, 2-Cl

The basic compound, 2,3-diazabicyclo[2.2.1]hept-5-ene, has proved very unstable, and thus difficult to prepare. This meant that its ^1H NMR spectrum was not published until 1993.[20] However, its *N*,*N*′-disubstituted derivatives are more stable and have been used in several studies to elucidate the double nitrogen inversions.[13,14] When the two *N*,*N*′ substituents are methyl groups the energetically more stable (12 kJ mol^{-1}) *trans* configuration with staggered conformation shows only one methyl signal: a somewhat broadened multiplet for the bridgehead protons and a triplet for the vinylic protons. This means that the inversion of the nitrogen atoms and interconversion of the two identical dimethyl derivatives is fast on NMR time scale.[13] Actually, the temperature has to be lowered to −39 °C for separate sharp peaks to be seen for each proton. Structural features may slow down or hinder the inversion so that an NMR spectrum for each configuration can be measured. In the present case we have two vicinal hydrogen atoms containing a heterocyclic ring in a strained bicyclo[2.2.1]hept-5-ene skeleton. In the compounds **1** the double nitrogen inversion is hindered by two bulky substituents, $COOCH_2CH_3$ and CONHAr. This can be observed by inspecting the proton spectra, which show separate peaks for each proton. Each signal also has analysable coupling constants. These spectra present an energetically more favourable *trans* configuration, which seems to be rather stable at room temperature.

The proton spectrum analysed for compound **1e** (EPOC, Table 1) shows that the geometry of the substituents attached to the two nitrogen atoms (N_2 and N_3) strongly affects the vicinal coupling constant values

Table 2. ^{1}H NMR chemical shifts (ppm) in $CDCl_3$ for compounds **1**

Proton	**1a**[a]	**1b**[b]	**1c**[c]	**1d**[d]	**1e**	**1f**	**1g**	**1h**	**1i**
H_1	5.08	5.10	5.09	5.10	5.10	5.09	5.09	5.10	5.13
H_4	5.32	5.34	5.33	5.34	5.33	5.32	5.32	5.32	5.36
H_5	6.57	6.59	6.58	6.60	6.59	6.59	6.59	6.59	6.62
H_6	6.52	6.53	6.51	6.53	6.52	6.52	6.53	6.50	6.57
H_7	1.74	1.76	1.75	1.77	1.74	1.76	1.77	1.79	1.83
H_7	1.74	1.76	1.75	1.77	1.74	1.77	1.76	1.76	1.79
H_{10}	7.84	7.85	7.88	7.89	7.96	8.06	8.05	8.18	8.65
H_{11}	4.25	4.27	4.26	4.28	4.27	4.27	4.27	4.29	4.31
H_{12}	1.30	1.31	1.34	1.32	1.31	1.31	1.31	1.33	1.34
$H_{2'}$	7.33	7.30	7.33	7.28	7.42	7.38	7.33	7.68	7.63
$H_{3'}$	6.81	7.08	7.10	–	7.27	7.22	7.37	–	8.15
$H_{4'}$	–	–	–	6.86	7.03	–	–	–	–
$H_{5'}$	6.81	7.08	7.10	7.16	7.27	7.22	7.37	7.30	8.15
$H_{6'}$	7.33	7.30	7.33	7.20	7.42	7.38	7.33	7.24	7.63

[a] X=OCH_3, 3.74 ppm.
[b] X=CH_3, 2.28 ppm.
[c] X=CH_2, 2.58 ppm; CH_3, 1.19 ppm.
[d] X=CH_3, 2.31 ppm.

between bridgehead and bridge methylene protons; for H_1 these are $^{3}J_{1,7a} = 0.86$ Hz and $^{3}J_{1,7b} = 2.33$ Hz, whereas for H_4 they are almost equal in size $^{3}J_{4,7a} = 1.58$ Hz and $^{3}J_{4,7b} = 1.55$ Hz.

The aromatic ring substituents clearly influence the shielding of the diaza nitrogen atoms N_2 and N_3 over seven bonds. The ^{15}N NMR chemical shift values collected in Table 4 show that when the aromatic ring is unsubstituted, or substituted with a 4-alkyl group, the shielding/deshielding effect in N_2 and N_3 is similar, but all the other substituents have a different size effect on the ring nitrogen atoms.

The investigation of the crystal packing of structures of **1a**, **1e**, **1f**, **1g** and **1i** reveals both intra- and intermolecular hydrogen bonding stabilizing the conformation of the compounds and on the other hand the packing of molecules to continuous chains (**1e**) or dimeric pairs (**1a**, **1f**, **1g** and **1i**) in the solid state. Compounds **1a**, **1f**, **1g** and **1i** pack into dimeric pairs, which are stabilized by doubled intermolecular hydrogen bonds between N_{10} and O_9 of the adjacent molecules (Fig. 1). In all the structures the intermolecular hydrogen bonds are almost the same length, being on average 3.08 Å (EPOC, Table 2). The difference between the hydrogen bonding schemes of these four crystal structures is observed when intramolecular hydrogen bonds are investigated. In **1a** an intramolecular hydrogen bond, which is substantially stronger than the intermolecular hydrogen bonding. In **1f** an intramolecular hydrogen bond of length 3.068(2) Å is formed between N_{10} and the ester oxygen O_{10}, whereas in

Table 3. ^{13}C NMR chemical shifts (ppm) in $CDCl_3$ for compounds **1**

Carbon	**1a**[a]	**1b**[b]	**1c**[c]	**1d**[d]	**1e**	**1f**	**1g**	**1h**	**1i**
C_1	65.23	65.47	65.37	65.50	65.42	65.46	65.46	65.55	65.57
C_4	64.30	64.49	64.42	64.48	64.38	64.28	64.46	64.26	64.15
C_5	137.38	137.72	137.58	137.74	137.58	137.51	137.73	137.54	137.28
C_6	136.32	136.46	136.43	136.41	136.46	136.32	136.74	136.65	136.72
C_7	47.50	47.78	47.67	47.80	47.69	47.70	47.92	47.76	47.70
C_8	159.28	159.38	159.28	159.35	159.23	159.12	159.28	159.01	158.62
C_9	160.01	160.32	160.20	160.34	160.21	160.19	160.40	160.24	160.13
C_{11}	62.79	63.10	62.98	63.15	63.03	63.11	63.33	63.26	63.26
C_{12}	14.11	14.36	14.24	14.35	14.24	14.24	14.46	14.27	14.09
$C_{1'}$	131.08	135.51	135.62	138.65	138.02	136.78	137.73	137.81	144.29
$C_{2'}$	121.05	119.45	119.43	119.97	119.26	120.46	120.99	120.80	118.23
$C_{3'}$	113.77	129.26	127.97	137.97	128.64	128.59	131.75	132.36	124.60
$C_{4'}$	155.71	132.95	139.33	124.25	123.30	128.12	115.89	126.20	142.35
$C_{5'}$	113.77	129.26	127.97	128.59	128.64	128.59	131.75	130.10	124.60
$C_{6'}$	121.05	119.45	119.43	116.43	119.26	120.46	120.99	118.51	118.23

[a] X=OCH_3, 55.11 ppm.
[b] X=CH_3, 20.64 ppm.
[c] X=CH_2, 2.58 ppm; CH_3, 1.19 ppm.
[d] X=CH_3 21.32 ppm.

Table 4. ^{15}N NMR chemical shifts (ppm) in $CDCl_3$ for compounds **1**

Nitrogen	**1a**	**1b**	**1c**	**1d**	**1e**	**1f**	**1g**	**1h**	**1i**[a]
N_2	−244.4	−244.1	−244.3	−244.0	−244.2	−243.9	−244.0	−243.8	−243.8
N_3	−244.7	−244.1	−244.3	−244.1	−244.2	−243.8	−243.9	−243.6	−242.5
N_{10}	−272.7	−270.6	−270.6	−269.8	−269.7	−270.9	−270.6	−271.0	−266.6

[a] X=NO_2, 12.3 ppm.

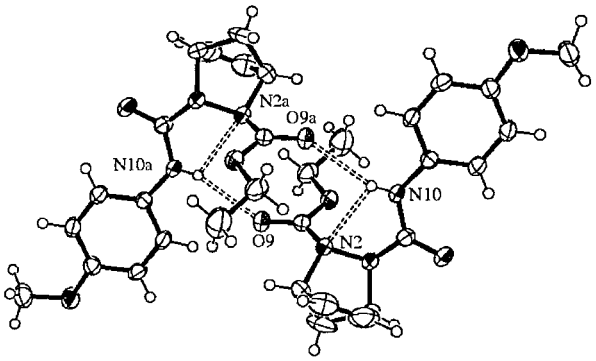

Figure 1. The ORTEP-III graph of the X-ray crystal structure of dimeric pair compound **1a**

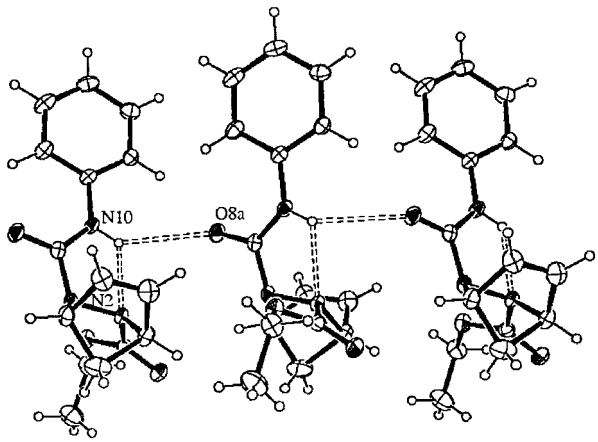

Figure 2. The ORTEP-III graph of the X-ray crystal structure of hydrogen bonds of the compound **1e**

1g there are no intramolecular hydrogen bonds at all. The 'maximized' intramolecular hydrogen bonding is observed in **1i**: there are two intramolecular hydrogen bonds from N_{10}, one to N_2 and the other to the ester oxygen O_{10}. Steric reasons are the cause for the hydrogen bond $N_{10}\cdots N_2$ being shorter than $N_{10}\cdots O_{10}$ [2.709(2) Å and 3.053(2) Å respectively].

The packing of **1e** is not dimeric-type packing, instead the molecules form continuous chains *via* weak intermolecular hydrogen bonds [$r(N_{10}\cdots O_{8*}) = 3.396(2)$ Å] (Fig. 2). Again, the intramolecular hydrogen bonding is much stronger than the intermolecular, the hydrogen bonding distance being 2.621(2) Å between N_{10} and N_2.

To study the electronic structure, geometry and preferential conformation of compounds **1**, semi-empirical AM1 data were calculated using standard parameterization.[21] Generally, 16 different possible conformations were considered regarding the mutual orientation of the diazabicycloheptene skeleton and the substituents attached to the N_2 and N_3 atoms. However, with regard to the mutual orientation of the C=O bonds and N—H bond, four optimized conformations **A**–**D** can be obtained for the parent molecule **1e** (see Scheme 2). As in the case of the previously studied ethyl 2-arylcarbamoyl-4,5-dimethyl-1,2,3,6-tetrahydropyridazine-1-carboxylates,[11,12] however, only the most stable conformations **A** and **B** are chosen for further discussion, since the conformations **C** and **D** have approximately 25 kJ mol^{-1} higher heat of formation ΔH_f values than **A** and **B**. Further, it appeared that the energetically most stable conformation is **B**. However, there is only a small difference (2.9 kJ mol^{-1}) in ΔH_f values between conformations **A** and **B**. The geometrical parameters of conformation **A** fit satisfactorily the experimental results of the X-ray analysis (see Table 5 and Fig. 4); in conformation **B**, however, there is an intramolecular hydrogen bond N_{10}—H$\cdots$O=C_9, the calculated interatomic distance H$\cdots$O being 2.1 Å. The selected AM1 atomic charges and bond orders are listed in the supplementary material (EPOC, Table 3).

The statistical results of the correlation of IR and NMR spectral data with substituent constants and AM1 semi-empirical bond orders and atomic charges are shown in Table 6. The wavenumbers of the stretching vibrations of both the C=O and N—H groups correlate with the Hammett σ constants of substituents X (except for ν(C=O) in CCl_4). The same is true for the correlation between the IR stretching vibrational wavenumbers and the calculated bond orders and atomic charges for conformation **B** (except for ν(C=O) in CCl_4). From the NMR results, only the chemical shifts of H_{10}, C_8, $C_{1'}$ and N_3 nuclei show satisfactory correlations with the Hamett σ parameters and corresponding atomic charge densities. In these correlations, in some cases the data for

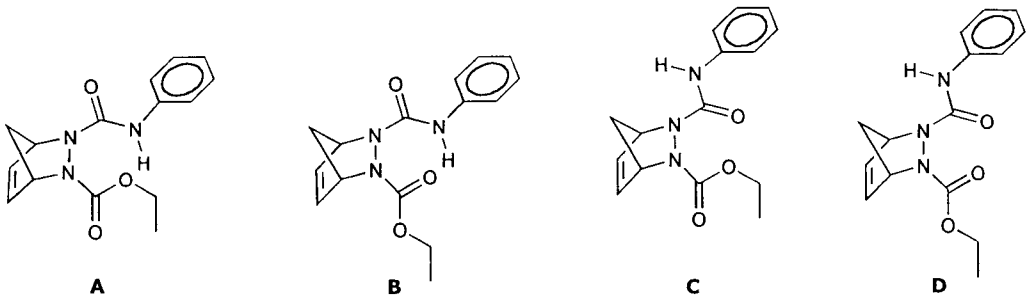

Scheme 2

Table 5. Comparison of X-ray and calculated structural data for compounds **1e** and **2** (X = 4-CH_3)[a]

	1e		**2** (X = 4-CH_3)[b]	
	X-ray	AM1	X-ray	AM1
Interatomic distances r (Å)				
$r(N_2—N_3)$	1.452(2)	1.416	1.405(2)	1.380
$r(C_1\cdots O_8)$	2.940(3)	2.896	2.914(3)	2.887
$r(H_{10}\cdots O_9)$	3.705(3)	3.843	3.88(2)	3.806
$r(C_{11}\cdots N_2)$	3.602(3)	3.679	3.588(3)	3.707
$r(N_{10}\cdots N_2)$	2.621(3)	2.895	2.687(2)	2.854
$r(N_{10}\cdots C_9)$	3.384(3)	3.414	3.316(2)	3.321
$r(O_8\cdots O_9)$	5.621(2)	5.748	5.352(2)	5.349
$r(C_1\cdots C_9)$	4.677(3)	4.732	4.464(3)	4.633
$r(C_8\cdots C_9)$	3.342(3)	3.380	3.160(2)	3.124
$r(H_7\cdots O_8)$	4.560(3)/4.976(3)[c]	4.655/4.944[c]	–	–
Angles ϑ (°)[d]				
$\vartheta(N_2—N_3—C_9)$	115.2(2)	118	120.2(1)	119
$\vartheta(N_3—N_2—C_8)$	115.7(2)	117	118.8(1)	120
$\vartheta(C_8—N_3—N_2—C_9)$	107.5(2)	110	79.7(1)	65

[a] Compounds **1** and **2** are in the same conformation **A**.
[b] Data calculated on the basis of results in Ref. 12
[c] For the second bridgehead hydrogen atom.
[d] The calculated bond angles are accurate to ±3° and the rotation angles to ±14°.

Table 6. Correlation of IR and NMR spectral data with empirical and theoretical values[a] ($y = \rho x + q$)

y	x	n	r	s	F	ρ	q
$\nu(C_8=O)$[b]	σ	9	0.919	1.45	38	8.46	1687.4
$\nu(C_8=O)$[c]	σ	9	0.849	0.84	18	3.41	1698.2
$\nu(C_9=O)$[c]	σ	9	0.940	1.03	53	7.15	1726.4
$\nu(N_{10}—H)$[b]	σ	9	0.967	1.32	102	−12.64	3411.4
$\nu(N_{10}—H)$[c]	σ	9	0.985	0.79	234	−11.54	3425.6
$\delta(C_{1'})$	σ	8[d]	0.788	2.29	11	7.35	136.3
$\delta(H_{10})$	σ	8[d]	0.963	0.08	77	0.75	8.0
$\delta(N_{10})$	σ	8[d]	0.828	1.04	13	4.12	−270.5
$\delta(N_2)$	σ	9	0.876	0.11	23	0.50	−244.1
$\delta(N_3)$	σ	8[d]	0.962	0.19	75	1.80	−244.1
$\nu(C_8=O)$[b]	$p(C_8=O)$	9	0.973	0.85	122	622.4	620.7
$\nu(C_8=O)$[c]	$p(C_8=O)$	9	0.926	0.61	42	258.2	1255.7
$\nu(N_{10}—H)$[b]	$p(N_{10}—H)$	9	0.972	1.22	121	2130.0	1546.7
$\nu(N_{10}—H)$[c]	$p(N_{10}—H)$	9	0.977	0.99	148	1919.5	1745.1
$\nu(C_8=O)$[b]	$q(C_8)$	9	0.976	0.80	139	1340.9	1186.7
$\nu(C_8=O)$[b]	$q(O_8)$	9	0.970	0.89	113	819.0	1995.6
$\nu(C_8=O)$[c]	$q(C_8)$	9	0.934	0.57	48	559.7	1489.2
$\nu(C_8=O)$[c]	$q(O_8)$	9	0.931	0.58	45	342.5	1827.1
$\nu(N_{10}—H)$[b]	$q(N_{10})$	9	0.857	2.68	19	1481.6	3846.1
$\nu(N_{10}—H)$[b]	$q(H_{10})$	9	0.974	1.19	128	−1432.1	3790.1
$\nu(N_{10}—H)$[c]	$q(N_{10})$	9	0.858	2.40	20	1329.3	3815.6
$\nu(N_{10}—H)$[c]	$q(H_{10})$	9	0.979	0.95	163	−1291.2	3767.0
$\delta(C_{1'})$	$q(C_{1'})$	9	0.956	1.09	75	128.3	127.2
$\delta(C_8)$	$q(C_8)$	9	0.901	0.110	30	−85.3	191.1
$\delta(H_{10})$	$q(H_{10})$	9	0.977	0.06	144	75.4	−12.0
$\delta(N_2)$	$q(N_2)$	9	0.895	0.10	28	−197.5	−277.5
$\delta(N_3)$	$q(N_3)$	9	0.866	0.33	21	572.7	−144.4
$\delta(N_{10})$	$q(N_{10})$	8[d]	0.907	0.78	28	−519.5	−423.1

[a] n is number of compounds used in the correlation, r is the correlation coefficient, s is the standard deviation of the slope and F is the Fisher–Snedecor test for parameters significant at the 95% level.
[b] In $CHCl_3$.
[c] In CCl_4.
[d] Compound **1h** omitted.

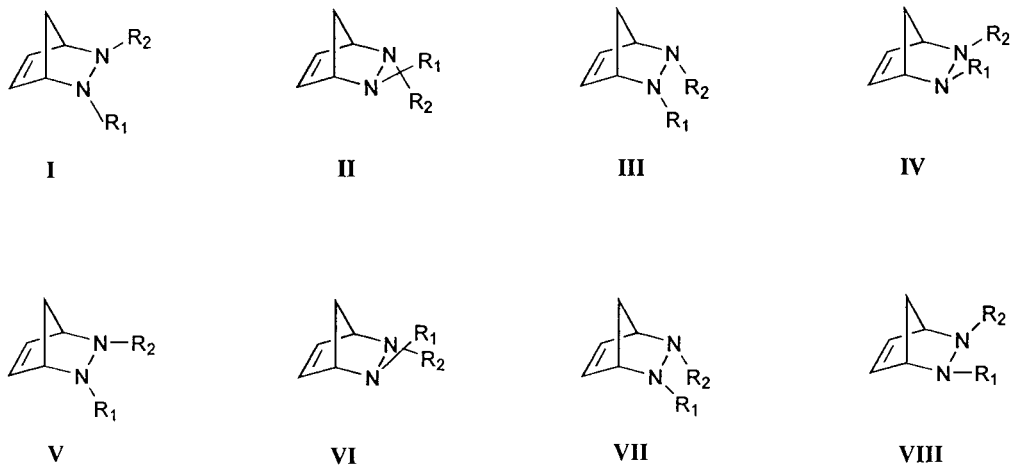

Scheme 3

the 3,4-disubstitued derivative (**1h**) were rejected as outliers. Comparison of the slopes of the linear correlations suggests that, in contrast to previously investigated disubstitued tetrahydropyridazines (**2**), in compounds **1** the electronic effects are transmitted more readily to the remote ester C_9=O group than to the vicinal amide C_8=O group. This can be explained by the preference of conformation **B** to be stabilized by an intramolecular hydrogen bond, but also by a more efficient transmission of substitutent effects *via* the small five-membered ring in **1** compared with that in the six-membered tetrahydropyridazine ring of **2**. The existence of the hydrogen-bonded structure **B** is also strongly supported by the aforementioned decrease of the $\nu(C_9{=}O)$ wavenumbers with respect to those for the monocyclic analogues **2**, in which a conformation without intramolecular hydrogen bonding but similar to structure **B** is preferred.[11]

Anderson and Lehn investigated the mechanism of interconversion of two optical antipodes of 2,3-dimethyl-2,3-diazabicyclo[2.2.1]hept-5-ene using temperature-dependent NMR spectra.[13] Our semi-empirical AM1 conformational calculations led to results that are in very good agreement with the experimental results reported.[13] Since compounds **1** are very similar to 2,3-dimethyl-2,3-diazabicyclo[2.2.1]hept-5-ene, using the AM1 method we decided to study the mechanism of their interconversion, which in fact corresponds to the inversion of the two nitrogen atoms N_2 and N_3. For preferential conformation **B** of the parent compound **1e**, eight optimized forms **I–VIII** (see Scheme 3) can be obtained by this inversion. The calculated ΔH_f values and the geometrical parameters of these forms are listed in the supplementary material (EPOC, Table 4). The forms **I** and **II** correspond to the energetical minima, whereas the forms **III** and **IV** have energies that are 25 kJ mol^{-1} higher. The energetical maxima belong to the 'half-planar' forms (conformations) **V–VIII** (where one of the nitrogen sites is nearly planar) and correspond to the transition states of double nitrogen inversion. The transition states were tested by one negative eigenvalue of the Hessian matrix.[21] The interconversion **I** ⇌ **II** may proceed in two ways, depending on which nitrogen site the inversion begins. If the inversion of form **I** begins on the N_2 nitrogen site, then the mechanism **I** ⇌ **VIII** ⇌ **IV** ⇌ **VI** ⇌ **II** might be considered. The potential curve of this conversion is presented in Fig. 3A and is similar to that obtained by us for 2,3-dimethyl-2,3-diazabicyclo[2.2.1]-hept-5-ene by AM1 calculation. On the other hand, if the inversion begins at the N_3 nitrogen atom, then the occurrence of mechanism **I** ⇌ **V** ⇌ **III** ⇌ **VII** ⇌ **II** can be expected (see Fig. 3B). In the first case the transgression of the transition state requires an energy of 32 kJ mol^{-1} and in the second case an energy of 28 kJ mol^{-1}. Since this energy difference is relatively small it cannot be anticipated which of these two mechanism is the preferred one. However, it can be concluded, on the basis of the preceding discussion and owing to the bulkiness of the substituents attached to the ring nitrogen atoms N_2 and N_3, that in compounds **1** a consecutive inversion process takes place, i.e. in which the two nitrogen atoms invert one after the other.

EXPERIMENTAL

General procedures for the synthesis of starting substituted hydrazines have been described.[22,23] Ethyl 3-arylcarbamoyl-2,3-diazabicyclo[2.2.1]hept-5-ene-2-carboxylates **1a–1i** were synthesized by using the following procedure: a solution of lead(IV) acetate (25 mmol) in dichloromethane (50–100 ml) was slowly added to a stirred and cooled (water, 4 °C) suspension of the corresponding substituted hydrazine (25 mmol) in dichloromethane (100–200 ml) and freshly distilled 1,3-cyclopentadiene (25 mmol). Stirring was continued at room temperature until the yellow or orange–red colour disappeared (4–24 h). The solid formed was collected by filtration and the solvent was washed with water, 0.1 M

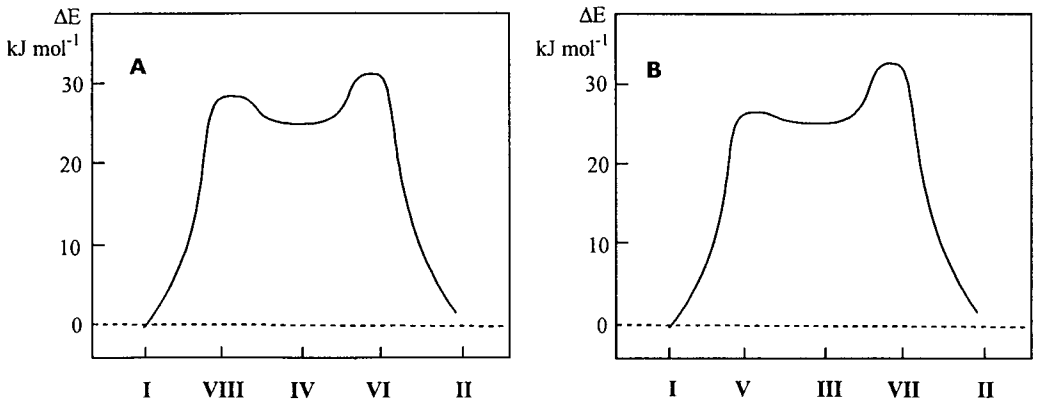

Figure 3. The potential curve for consecutive double nitrogen inversion of compound **1e** obtained from values calculated by the AM1 method: **A** mechanism **I** ⇌ **VIII** ⇌ **IV** ⇌ **VI** ⇌ **II**; **B** mechanism **I** ⇌ **V** ⇌ **III** ⇌ **VII** ⇌ **II**

sodium hydroxide, 0.1 M nitric acid and again with water. After drying with sodium sulfate the solvent was removed under reduced pressure. The residue was purified by recrystallization from ethanol, ethanol–water or ethanol–*n*-hexane. The characteristic data of the newly prepared compounds are listed in the supplementary material (EPOC, Table 5). The compositions of the compounds were in satisfactory agreement with the results of elemental analysis (C, H, N). The structures of the substances were confirmed using ^{1}H NMR, ^{13}C NMR, IR and mass spectra.

The FTIR spectra were measured on a Bruker IFS 25 spectrometer at room temperature using NaCl cells of 0.5 and 3.2 mm thickness. The concentration of the solutions varied in the range of 1–5 mg cm^{-3} in both solvents CCl_4 and $CHCl_3$ (Uvasol, Merck). Peak positions were determined with an accuracy of ± 0.1 cm^{-1} after deconvolution and separation of absorption bands in the region of the C=O and C=C stretching vibrations. The band positions were fitted using Lorenz–Gaussian sum functions.

The ^{1}H, ^{13}C and ^{15}N spectra were recorded for 0.5 mol $CDCl_3$ solution in a 5 mm sample tube at 30 °C on a Bruker Avance DRX500 spectrometer working at 500.13 MH_3, 125.77 MH_3 and 50.69 MHz respectively. In the ^{1}H NMR experiments the number of data points was 64K, giving a spectral resolution of 0.05 Hz; the number of scans was eight and the flip angle was 30°. An exponential window function of the spectral resolution was used prior to Fourier transformation. The ^{1}H NMR chemical shifts are referenced to the signal of residual $CHCl_3$ [$\delta = 7.26$ ppm from tetramethylsilane (TMS)]. In the ^{13}C NMR experiments the number of data points was 32K, giving a spectral resolution of 0.5 Hz; the number of scans was 64 and the flip angle was 30°. A composite pulse decoupling, Waltz-16, was used to remove proton couplings. An exponential window function of the spectral resolution was used prior to Fourier transformation. The ^{13}C NMR chemical shifts are referenced to the central peak of $CDCl_3$ ($\delta = 77.00$ ppm from TMS). The ^{15}N NMR chemical shifts are referenced to external CH_3NO_2 ($\delta = 0.0$ ppm). The number of data points in PFG ^{1}H–^{13}C HMQC[24,25] and HMBC[26] measurements was $1024(f_2) \times 512(f_1)$. This matrix was zero filled to 2048×1024 and apodized by a shifted sine bell window function along both axes before Fourier transformation. For PFG ^{1}H–^{15}N HMBC experiments a 50 ms delay was used for evolution of long-range couplings. The number of the data points was $1024(f_2) \times 512$ ppm ($f_1 = {}^{15}$N). This matrix was zero filled to 1024×1024 and apodized by a shifted sine bell window function along both axes before fourier transformation.

The X-ray crystallographic data for compounds **1a, 1e, 1f, 1g** and **1i** were recorded with a Nonius Kappa CCD diffractometer using graphite monochromatized *Mo Kα* radiation [$\lambda(Mo\ K\alpha) = 0.710\ 73$ Å] at a temperature of 173.0 ± 0.1 K. The data were processed with Denzo-SMN v0.93.0[27] and all structures were solved by direct methods (SHELXS-97)[28] and refined on F^2 by full-matrix least-squares techniques (SHELXL-97).[29] The hydrogen atoms were located from the difference Fourier map and refined with isotropic temperature factors (1.2 times the

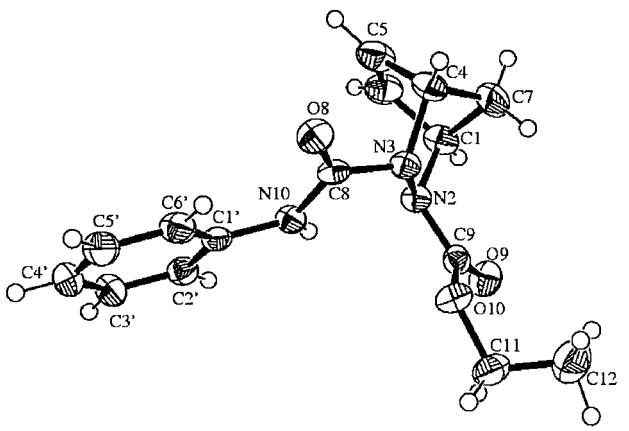

Figure 4. The ORTEP-III graph kof the X-ray crystal structyure of compound **1e**.

carbon temperature factor). The absorption correction was applied but not used in the final refinement, since it had an unfavourable effect on the quality of the structure. Suitable crystals for X-ray analysis were obtained from slow evaporation of $CDCl_3$. The experimental crystallographic data and structure refinement details are listed in the supplementary material (EPOC, Table 6). The representative ORTEP-III graph[30] for compound **1e** is shown in Fig. 4 and the graphs for compounds **1a, 1f, 1g** and **1i** are given in the supplementary material (EPOC, Figs 1–4.

Crystallographic data (excluding structure factors) for the structures reported in this paper have been deposited with the Cambridge Crystallographic Data Centre as supplementary publication nos CCDC-165232–CCDC-165236. Copies of the data can be obtained free of charge on application to CCDC, 12 Union Road, Cambridge CB2 1EZ, UK.

Acknowledgements

The authors appreciate the financial support of both the International Bureau of the 'Bundesministerium für Bildung und Forschung beim DLR' in Bonn (project no.: SVK-98/003) and the Slovak Ministry of Education (project no. Nem/SLA – 00318), as well as the donations of the Scientific Grant Agency of Ministry of Education of Slovak Republic (grant no. 1/7399/20). The authors are also grateful to Mrs I. Schaller from the Institute of Physical Chemistry, Martin Luther University in Halle (Saale), Germany, for the measurement of the FTIR spectra.

REFERENCES

1. Kornet MJ, Daniels R. *J. Heterocycl. Chem.* 1980; 1465.
2. Kam S-T, Hanson RN, Porthogese PS. *J. Pharm. Sci.* 1980; **69**: 1007.
3. Riemschneider R. *Z. Angew. Entomol.* 1961; **48**: 301.
4. Boger DL, Weinreb S. In *Hetero Diels–Alder Methodology in Organic Synthesis*. Academic Press, Inc.: San Diego, 1987; 154–166.
5. Furdík M, Mikulášek S, Priehradný S. *Acta Fac. Rer. Nat. Univ. Comen., Ser. Chim.* 1967; **12**: 239.
6. Bock H. *Angew. Chem.* 1965; **77**: 469; *Angew. Chem., Int. Ed. Engl.* 1965; **4**: 457.
7. Bock H, Kroner J. *Chem. Ber.* 1966; **99**: 2039.
8. Knight GT, Loadman MJR, Saville B, Wildgoose J. *J. Chem. Soc., Chem. Commun.* **1973**: 193.
9. Gölz H, Glatz B, Haas G, Helmchen G, Muxfeldt H. *Angew. Chem.* 1977; **89**: 742; *Angew. Chem., Int. Ed. Engl.* 1977; **16**: 728.
10. Cremlyn RJW, Freason MJ, Milnes DR. *Phosphorus* 1976; **6**: 207.
11. Perjéssy A, Meyer P, Rudorf W-D, Loos D, Kolbe A, Schaller I. *Heterocycl. Commun.* 1999; **5**: 127.
12. Kolehmainen E, Laihia K, Nissinen M, Pihlaja K, Perjéssy A, Loos D, Rudorf W-D, Meyer P. *J. Chem. Res. (S)* 1999; 186; *J. Chem. Res. (M)* 1999; 0933.
13. Anderson JF, Lehn J-M. *J. Am. Chem. Soc.* 1967; **89**: 81.
14. Anderson JF. *J. Am. Chem. Soc.* 1969; **91**: 6374.
15. Rudorf W-D, Meyer P. Unpublished results.
16. Wakabayashi O, Matsutani K, Ota H, Naohara T, Suzuki S. *Japan Kokai* 77 83,687 (12 July 1977); *Chem. Abstr.* 1977; **87**: 201548e.
17. Wakabayashi O, Matsutani K, Ota H, Naohara T, Watanabe H. *Japan Kokai* 78 40,785 (13 April 1978); *Chem. Abstr.* 1978; **89**: 180031e.
18. Linker K-H, Findeisen K, Schallner O, Lender A, Santel H-J, Dollinger M, Yanagi A, Goto T. *Ger. Offen*. DE 19,531,152 (20 August 1995);18*Chem. Abstr.* 1996; **125**: 142740q.
19. PERCH Software, Version 1/98, distributed by PERCH Project, Department of Chemistry, University of Kuopio, Kuopio, Finland.
20. Wang C-X, Sheridan RS. *Tetrahedron Lett.* 1993; **34**: 5673.
21. AMPAC 5.0, 1994 Semichem, 7128 Summit, Shawnee, KS 66216.
22. Cookson RC, Gupte SS, Stevens IDR, Watts CT. *Org. Synth.* 1971; **51**: 121.
23. Bollbuck G, Stroh HH, Barnikow G. *J. Prakt. Chem.* 1971; **313**: 773.
24. Bax A, Griffey RH, Hawkins BL. *J. Magn. Reson.* 1983; **65**: 301.
25. Bax A, Subramanian S. *J. Magn. Reson.* 1986; **67**: 565.
26. Bax A, Summers MF. *J. Am. Chem. Soc.* 1986; **108**: 2093.
27. Otwinowski Z, Minor W. In *Methods of Enzymology*, Vol. 276: *Macromolecular Crystallography, part A*, Carter Jr CW, Sweet RM (eds). Academic Press: 1997; 307–326.
28. Sheldrick GM. *Acta Crystallogr. J. Sect. A* 1990; **46**: 467.
29. Sheldrick GM. SHELXL-97—a Program for Crystal Structure Refinement, 1997, University of Göttingen, Germany.
30. Burnet MN, Johnson CK. ORTEP-III: Oak Ridge Thermal Ellipsoid Plot Program for Crystal Structure Illustrations, Oak Ridge National Laboratory ORNL-6895, 1996.